

Stochastic modelling of experimental chaotic time series

Thomas Stemler,* Johannes P. Werner, and Hartmut Benner
*Institute for Solid State Physics, Darmstadt University of Technology,
Hochschulstraße 6, D-64289 Darmstadt, Germany*

Wolfram Just[†]

Queen Mary / University of London, School of Mathematical Sciences, Mile End Road, London E1 4NS, UK
(Dated: August 21st, 2006)

Methods developed recently to obtain stochastic models of low-dimensional chaotic systems are tested in electronic circuit experiments. We demonstrate that reliable drift and diffusion coefficients can be obtained even when no excessive time scale separation occurs. Crisis induced intermittent motion can be described in terms of a stochastic model showing tunnelling which is dominated by state space dependent diffusion. Analytical solutions of the corresponding Fokker-Planck equation are in excellent agreement with experimental data.

PACS numbers: 05.45.Tp, 05.10.Gg, 05.40.-a

Keywords: intermittency, Fokker-Planck equation, electronic circuit experiment

Introduction – Modelling dynamical degrees of freedom by suitable stochastic forces is a classical subject in theoretical physics and applied mathematics. While the replacement of many degrees of freedom in a thermodynamic system by Gaussian white noise is a textbook example and the foundation of e.g. irreversible thermodynamics [1] it is quite a recent finding that few chaotic degrees of freedom can be modelled by stochastic differential equations (cf. e.g. [2] for a seminal reference in the context of climate research, or [3, 4] for a mathematical account). To some extent such approaches rely on the property that certain nice chaotic dynamical systems can be described rigorously in terms of Markov chains (cf. e.g. [5]). Meanwhile the modelling of chaotic dynamics by suitable stochastic systems has been applied in diverse contexts, e.g. for the confirmation of stochastic models in hydrodynamics [6], analysis of stock market data [7], or for climate models [8].

Above all, in theoretical terms such approaches rely on time scale separation such that irrelevant fast chaotic degrees of freedom can be described in terms of a noise process acting on slow relevant degrees of freedom. While in mathematical models time scale separation can be usually achieved by introducing some small parameter the situation may be less obvious in real experimental contexts, in particular when no established mathematical model is at hand like in nanoscience or biophysics. Nevertheless, even in these fields stochastic models seem to be quite successful [9–11]. Here we want to address the question to which extent time scale separation is crucial in order to model chaotic degrees of freedom by a noise process. Certain aspects of such a question might be answered by numerical simulations. But then one might suspect that the findings depend severely on the chosen model and are of limited relevance for real world applications. We therefore prefer to tackle the problem from the very beginning by real experiments. Our setup should be

simple so that experimental conditions can be controlled easily. We thus focus on electronic circuits. While one might suspect that certain aspects of such experiments cannot be generalised and the same limitations like in numerical simulations may apply, one has to keep in mind that several features in real experiments are universal, like the occurrence of internal dynamical and external measurement noise, the competition of these unwanted noise sources with the chaotic motion, drift of parameters, or limitations of the accessible observables and of the ensemble sizes. Thus experimental verification of stochastic modelling has higher predictive power than plain numerical analysis.

In formal terms we want to model a dynamical system, say a chaotic differential equation $\dot{\mathbf{x}} = \mathbf{f}(\mathbf{x})$, by a suitable Langevin equation. We suppose that we can measure just a scalar time series $z(t) = g(\mathbf{x}(t))$, e.g. a component of the state vector \mathbf{x} or a nonlinear function of the components. The essential features of the dynamics of $z(t)$ should be captured by a stochastic differential equation with Gaussian white noise source. Therefore, we need to estimate a suitable systematic part, i.e. a drift function $D_1(z)$, and a diffusion coefficient $D_2(z)$. There exists a standard recipe to obtain such quantities in terms of the first and the second moment [12]

$$\Delta t D_1(Z) = \langle (z(t + \Delta t) - z(t)) \rangle + o(\Delta t) \quad (1a)$$

$$2\Delta t D_2(Z) = \langle (z(t + \Delta t) - z(t))^2 \rangle + o(\Delta t) \quad (1b)$$

where the averages are conditional averages with the constraint $z(t) = Z$. While for a stochastic differential equation eqs.(1) yield the drift and diffusion in the asymptotic limit $\Delta t \rightarrow 0$ one has to observe that for the stochastic modelling of fast chaotic systems the delay Δt has to be large compared to the correlation time of the chaotic motion [13]. Apart from such a constraint eqs.(1) have to be evaluated in the asymptotic limit of small Δt . There is of course no a priori guarantee whether a modelling

in terms of the quantities (1) is a sufficient description, e.g. whether the dynamics of $z(t)$ can be described by a Markovian process or whether higher-order moments become relevant. These problems are in particular crucial when no pronounced time scale separation is available. Thus we have to check a posteriori to which extent such a stochastic description yields satisfactory results.

Experimental Setup – For our investigations we use a nonlinear autonomous electronic circuit design which was first introduced in [14]. A diagrammatic view of the circuit is shown in figure 1.

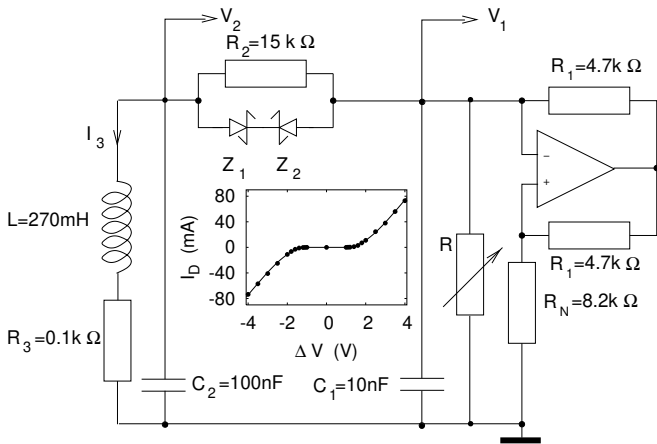


FIG. 1: Diagrammatic view of the Shinriki oscillator. Inset: experimental data (symbols) and analytical data fit (line) of the current-voltage characteristics of the two Zener diodes .

The device consists of an RLC circuit that is coupled to an RC element via a nonlinearity. The essential nonlinear element consists of two Zener diodes $Z_{1,2}$ (BZX85C3V3). The current-voltage characteristics of these diodes is shown in figure 1. Its shape is described by the expression $I_D(V_1 - V_2) = I_D(\Delta V) = \text{sgn}(\Delta V)f(|\Delta V| - V_Z)$ where $V_Z = (1.02 \pm 0.04)\text{V}$ and $f(x) = (Ax^2 + Bx^3)\Theta(x)$ denotes a third order fit with parameter values $A = (13.1 \pm 0.7)\text{mA/V}^2$ and $B = (-1.59 \pm 0.15)\text{mA/V}^3$. Parallel to the oscillating part of the circuit there is a negative impedance converter (NIC), consisting of an operational amplifier (Analog Devices AD711JN), two identical feedback resistors R_1 and a resistor R_N connected to ground. This NIC acts as a linear ‘negative resistor’ with the resistance $-R_N$ supplying the power for the circuit. The current supplied to the oscillatory part of the circuit can be controlled by variation of the adjustable resistor R . This variable resistor acts as the control parameter of the system. The other components of the circuit are fixed and the corresponding parameter values are contained in figure 1. We just mention that applying Kirchhoff’s rules to the circuit one easily obtains the equations of motion [15] but here we are not going to make use of such a mathematical model.

For data acquisition we used a transient recorder card

(Meilhaus ME2600) to measure the voltage V_1 . This card includes also several digital output channels which were used for on-line variation of the control parameter by means of several digital resistors (Xicor X9C102/4P) replacing the tunable resistor R . The fully computer controlled experiment enabled us to measure long time series for different control parameter values.

Increasing the control parameter the circuit shows the typical period doubling route to chaos. Beyond a critical control parameter value $R_c = 66\text{k}\Omega$ intermittency is observed. The intermittency results from an attractor merging crisis. Below the critical control parameter R_c two symmetric attractors can be found in the phase space of the system. The initial condition determines the state which is attained in the long time asymptotics. For control parameter values above R_c a new attractor occurs, consisting of the merged precritical attractors. The symmetry of the nonlinearity is essential for the bifurcation scenario. For the particular circuit this chaos-chaos intermittency scenario can be studied in detail over a wide range of control parameter values.

The observed dynamics in the intermittency regime can be characterised by fast oscillations on the precritical attractors and a slow jump dynamics between two repelling chaotic states (see figure 2). The typical period of the fast oscillations is of about $T_{osc} \sim 1.5\text{ms}$. The mean residence time τ in the two chaotic states depends on the difference between the actual and the critical control parameter, $\Delta R = R - R_c$. In our experiment we observed mean residence times from 0.1s at $\Delta R \approx 100\Omega$ to 3ms at $\Delta R \approx 8\text{k}\Omega$. Thus our experiment allows for a dynamical range of parameter values of about two orders of magnitude. Close to R_c the mean residence time obeys a typical scaling law [16] $\tau \sim \Delta R^{-\gamma}$ with a critical exponent of $\gamma \sim 0.7$ [15]. Above all, a superficial inspection of the time series shows a behaviour which resembles the motion of a bistable stochastic model. However, for typical parameter values of ΔR there are of about 10-100 oscillations on a chaotic saddle before a jump to the inverse image appears. Thus, time scales of the chaotic motion are not very well separated from the intermittent motion and it is far from obvious whether a bistable stochastic model captures the essential features of the time series.

Stochastic Model – We are now going to reconstruct an effective stochastic model from experimental data of the voltage $z(t) = V_1(t)$. A time series of 6×10^5 data points with sampling time $80\mu\text{s}$ is used to estimate the drift and the diffusion coefficient according to eqs.(1). The basic oscillation period is of the order of $T_{osc} \sim 1.5\text{ms}$ at $\Delta R = 1.1\text{k}\Omega$ while intermittent jumps take place on a time scale of order $\tau \sim 14T_{osc}$. Evaluation of eqs.(1) for different delays shows a plateau at an intermediate scale $\Delta t \in [2\text{ms}, 8\text{ms}]$ (cf. figure 3). Thus, such values can be used to estimate the parameters of our model.

Spatially resolved drift and diffusion functions have been estimated using $\Delta t = 4.5\text{ms}$. The conditional

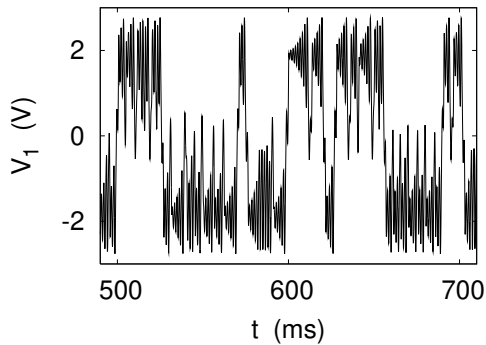


FIG. 2: Time series sample of $V_1(t)$ for $\Delta R = R - R_c = 1.1\text{k}\Omega$ measured with a sampling time of $80\mu\text{s}$. A time scale separation, although not very pronounced, between oscillatory motion $T_{osc} \sim 1.5\text{ms}$ and intermittent jumps $\tau \sim 20\text{ms}$ is visible.

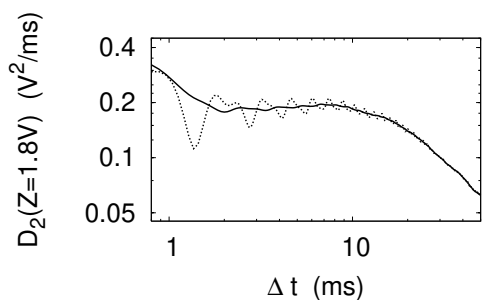


FIG. 3: Dependence of the second moment (cf. eq.(1b)) on the time delay Δt evaluated at $Z = V_1 = 1.8\text{V}$. Raw data (broken line), sliding average over one period T_{osc} (solid line). Control parameter $\Delta R = 1.1\text{k}\Omega$. A plateau appears for $\Delta t \in [2\text{ms}, 8\text{ms}]$ while for larger values of the delay the characteristic power law decay is observed.

averages are computed on a spatial grid with stepsize $\Delta Z = 50\text{mV}$ so that approximately each data point is generated by an ensemble of size 5×10^3 . The final results are rather robust against these choices. Figure 4 shows the data obtained at $\Delta R = 1.1\text{k}\Omega$. The drift is dominated by a linear decay with a superimposed oscillatory structure, while the diffusion has a unimodal shape being large in centre and small at the boundaries. The peak structure for $z = V_1 \in \pm[0.7\text{V}, 1.4\text{V}]$ seems to be an artifact generated by the spiky time series since no such feature shows up in the stationary distribution of the voltage (cf. inset in figure 4). The large scale features of drift and diffusion are stable with respect to the details of the time series analysis. Thus, despite of the lack of pronounced time scale separation the method yields reproducible drift and diffusion functions.

In order to test the accuracy of the results displayed in figure 4 we check whether the corresponding stochastic model predicts features of the dynamics, i.e. the mean

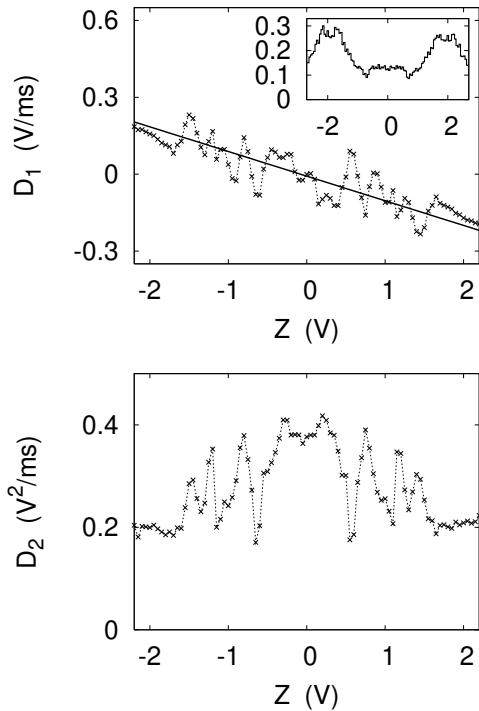


FIG. 4: Drift (top) and diffusion (bottom) evaluated for $\Delta t = 4.5\text{ms}$ at $\Delta R = 1.1\text{k}\Omega$, in dependence on the voltage $Z = V_1$ (cf. eqs.(1)). Conditional averages were computed with a spatial resolution $\Delta Z = 50\text{mV}$. The straight line indicates a least square fit in the interval $[-1.6\text{V}, 1.6\text{V}]$ to estimate the global trend of the drift. The inset shows the distribution of V_1 as a histogram with resolution $\Delta Z = 50\text{mV}$.

residence time τ which can be measured independently as well. It is of course a nontrivial task to obtain mean residence times for Fokker-Planck models with nontrivial drift and diffusion coefficients. For the sake of a simple analytical estimate let us model the drift and diffusion coefficients just by taking into account the essential features of the graphs displayed in figure 4. Therefore let us approximate the drift by a linear expression, $D_1(z) = -\alpha z$ neglecting the oscillating superstructure visible in the data, and the diffusion by a parabola $D_2(z) = D(z_0^2 - z^2)$. Although such an approximation seems to be quite crude, both expressions are simple, obey the symmetry of the system, and have the tremendous advantage that the corresponding Fokker-Planck equation

$$\frac{\partial \rho(z, t)}{\partial t} = \alpha \frac{\partial z \rho(z, t)}{\partial z} + D \frac{\partial^2 (z_0^2 - z^2) \rho(z, t)}{\partial z^2} \quad (2)$$

can be solved analytically. Actually, the stationary distribution of eq.(2) is given by $\rho_*(z) \sim (z_0^2 - z^2)^{\alpha/(2D)-1}$ showing a pronounced double peak structure for $\alpha < 2D$, while the eigenvalues of the Fokker-Planck operator which govern the time evolution read $\Lambda_n = -n\alpha - n(n-1)D$. Thus, there appears a spectral gap for $\alpha \ll D$ and

the stochastic model displays a slow jump process on the time scale $\tau = 2/\alpha$.

We employ such an analytical estimate by computing the linear trend α using a least square fit in the interval $[-1.6V, 1.6V]$. Hence, we can estimate the mean residence time of the stochastic model for different values of the control parameter ΔR . Comparison with direct observations yields a remarkable coincidence (cf. figure 5) and the theoretical prediction is quite accurate over a wide parameter range. We therefore conclude that our stochastic model, apart from some fine structure, captures quite well the intermittent features on the slow time scale.

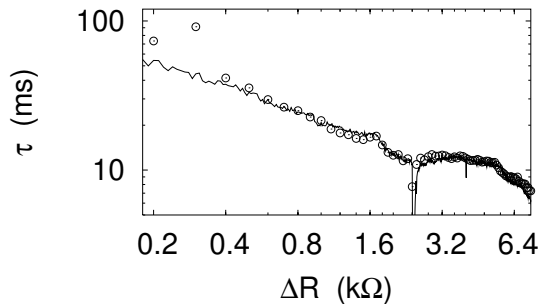


FIG. 5: Mean residence time τ in dependence on the control parameter ΔR . Line: experimental data from time series of lengths 48s recorded with stepsize 10Ω , symbols: analytical estimate obtained from the stochastic model (cf. eq.(2)).

Conclusion – We have demonstrated that even without a pronounced time scale separation one may successfully model chaotic dynamics by stochastic forces. Drift and diffusion coefficients can be constructed from experimental time series. The stochastic model is able to capture the essential features of the intermittent motion, i.e. the quantitative prediction of the mean residence time over a large parameter region. Although we do not have any proof that the restriction to second order moments is justified, the experimental results confirm that higher order moments and non-Markovian effects are of minor importance for the properties of the intermittent motion. Above all, such good agreement may stimulate further applications of stochastic modelling in experiments.

Our simple analytical estimate for the mean residence time was certainly too crude to capture all the details of the drift and diffusion coefficients. For instance, the analytical expressions model the chaotic repellers just by fixed points. But such a simplification allows for a complete analytical solution of the stochastic model. Such solution reveals the main mechanism of the intermittent dynamics. It is essentially modelled by the spatial dependence of the diffusion function, i.e. by multiplicative noise processes while the structure of a potential plays a minor role. Thus, the tunnelling in such a model is dominated by diffusion. That in fact fits with the underlying

chaotic dynamics which does not give rise to a bistable potential in an obvious way. But phase space dependent local Lyapunov exponents cause state dependent fluctuations.

In summary, modelling of chaotic motion by effective stochastic dynamics could have a wide range of applications even for systems without extreme time scale separation. The stochastic models may reveal features about the underlying nonlinear dynamics as well. Thus such modelling is more than just a practical tool. It might be used to uncover underlying physical mechanisms in real experiments as well.

* Electronic address: stemler@exp1.fkp.physik.tu-darmstadt.de

† Electronic address: w.just@qmul.ac.uk

- [1] S. R. de Groot and P. Mazur, *Non-equilibrium thermodynamics* (North-Holland, Amsterdam, 1969).
- [2] K. Hasselmann, *Stochastic climate models: part I. theory*, *Tellus* **28**, 473 (1976).
- [3] C. Beck, *From the Perron–Frobenius equation to the Fokker–Planck equation*, *J. Stat. Phys.* **79**, 875 (1995).
- [4] D. Givon, R. Kupferman, and A. Stuart, *Extracting macroscopic dynamics: model problems and algorithms*, *Nonl.* **17**, R55 (2004).
- [5] C. Robinson, *Dynamical systems : stability, symbolic dynamics, and chaos* (CRC Press, Boca Raton, 1995).
- [6] R. Friedrich and J. Peinke, *Description of a turbulent cascade by a Fokker–Planck Equation*, *Phys. Rev. Lett.* **78**, 863 (1997).
- [7] R. Friedrich, J. Peinke, and C. Renner, *How to quantify deterministic and random influences on the statistics of the foreign exchange market*, *Phys. Rev. Lett.* **84**, 5224 (2000).
- [8] A. Majda, I. Timofeyev, and E. Vanden-Eijnden, *Stochastic models for selected slow variables in large deterministic systems*, *Nonl.* **19**, 769 (2006).
- [9] F. Jülicher, A. Ajdari, and J. Prost, *Modeling molecular motors*, *Rev. Mod. Phys.* **69**, 1269 (1997).
- [10] A. Neiman and D. F. Russell, *Stochastic biperiodic oscillations in the electroreceptors of paddlefish*, *Phys. Rev. Lett.* **86**, 3443 (2001).
- [11] P. Reimann, *Brownian motors: noisy transport far from equilibrium*, *Phys. Rep.* **361**, 57 (2002).
- [12] H. Risken, *The Fokker–Planck equation : methods of solution and applications* (Springer, Berlin, 1989).
- [13] H. Kantz, W. Just, N. Baba, K. Gelfert, and A. Riegert, *Fast chaos versus white noise - entropy analysis and a Fokker–Planck model for the slow dynamics*, *Physica D* **187**, 200 (2004).
- [14] M. Shinriki, M. Yamamoto, and S. Mori, *Multimode oscillations in a modified Van der Pol oscillator containing a positive nonlinear conductance*, *Proc. IEEE* **69**, 394 (1981).
- [15] J. P. Werner, T. Stemler, and H. Benner, *Crisis and stochastic resonance in Shinriki’s circuit* (preprint), 2006.
- [16] C. Grebogi, E. Ott, and J. A. Yorke, *Crisis sudden changes in chaotic attractors and transient chaos*, *Physica D* **7**, 181 (1983).